Non-binary m-sequences for reliable, high-speed Brain–Computer Interfaces based on c-VEP: a pilot study

Víctor Martínez-Cagigal[1,2], Eduardo Santamaría-Vázquez[1,2] Sergio Pérez-Velasco[1], Diego Marcos-Martínez[1], Selene Moreno-Calderón[1], and Roberto Hornero[1,2]

[1] Biomedical Engineering Group, ETSIT, University of Valladolid, Valladolid, Spain
[2] Centro de Investigación Biomédica en Red de Bioingeniería, Biomateriales y Nanomedicina (CIBER-BBN), Spain

Abstract. Code-modulated visual evoked potentials (c-VEPs) can provide reliable, high-speed communication for non-invasive brain-computer interfaces (BCIs). Most studies use shifted versions of binary m-sequences to encode the commands, i.e., flashing black and white targets according to the shifted code. Despite excellent performances, high-contrast stimuli cause eyestrain for some users. In this work, we studied the possibility of using m-sequences with non-binary bases, encoded with different shades of gray, as a more pleasant alternative. A c-VEP-based online BCI at a 120 Hz refresh rate was tested with 3 subjects using base 2 (63-bit), base 3 (80-bit), base 5 (124-bit), and base 11 (120-bit) m-sequences. Raster latencies correction and an online artifact rejection approach were applied. Results showed that all subjects were able to achieve perfect accuracy using all bases (base 2: 100%, 2.1 s/trial, 114.3 bpm; base 3: 100%, 2.6 s/trial, 90.0 bpm; base 5: 100%, 3.1 s/trial, 77.4 bpm; base 11: 100%, 8.0 s/trial, 30 bpm). Furthermore, p-ary m-sequences were perceived as 15.28% (base 3), 45.88% (base 5), and 51.39% (base 11) less obtrusive in relative percentage than the binary sequence. These preliminary results suggest that non-binary sequences may be more comfortable for users without degrading system accuracy.

Keywords: non-binary codes, visual evoked potential (VEP), code-modulated VEP (c-VEP), brain–computer interface (BCI), electroencephalography (EEG)

1 Introduction

The ability of brain–computer interfaces (BCIs) to provide a direct pathway between user's brain activity and external devices makes them suitable systems to replace or even restore central nervous system outputs [1]. In this context, BCIs have been traditionally perceived as powerful potential alternative and augmentative communication (AAC) technologies to improve the quality of life of motor-disabled patients [1]. These non-invasive BCIs monitor the electroencephalographic (EEG) signals of the user to decode their intentions in real-time and translate them into commands that control applications or external devices [1].

Control signals such as P300 evoked potentials or steady-state visual evoked potentials (SSVEP) have been extensively used in the literature to implement BCI spellers, reaching suitable accuracies and information transfer rates (ITR), e.g., approx. $> 90.0\%$ at 10–25 bpm (P300) [2,3] or 40–50 bpm (SSVEP) [4,5] for healthy users. Recently, code-modulated VEPs (c-VEP) have been proposed as a novel control signal that can outperform both P300 and SSVEP-based approaches in terms of performance and calibration times [6]; e.g., 91.0% at 92.8 bpm [4], 94% at 92.7 bpm [5].

In a classical circular-shifting c-VEP paradigm, a template is calibrated using the EEG response of the user when paying attention to a visual stimuli that flickers following a pseudo-random noise code. Then, different commands are encoded with shifted versions of this code, allowing identification of the command the user is looking at by correlating the EEG response with these shifted templates [6]. To favor the classification, the pseudo-random code should present low auto-correlation values for non-zero circular shifts, so that other commands can use delayed versions of the code without incrementing the risk of misclassifications. Usually, binary maximal length sequences (i.e., m-sequences) are used due to their excellent auto-correlation properties; i.e., encoding commands using black (0) or white (1) flashings [6].

Despite the excellent performances achieved using binary m-sequences to encode commands, it has been reported that its high-contrast stimuli cause eyestrain for some users, especially for low refresh rates [6]. Thus, a necessary step toward plug-and-play implementations of c-VEP-based BCIs in real environments should be aimed at reducing the discomfort of the flickering as long as possible. On the one hand, there is a consensus that the higher the presentation rate (i.e., the sampling rate of the code), the less fatiguing the stimulation is for the user [6]. Although most c-VEP-based studies flicker at 60 Hz, presentation rates of 120 Hz are recommended, which provide shorter calibration and selection times while maintaining suitable selection accuracy [6]. Noteworthy, higher presentation rates than 120 Hz are discouraged, since c-VEP templates become less orthogonal to each other [7]. On the other hand, some studies opted to customize the pseudo-random noise code. Several authors proposed hand-crafted codes that confine spectral density to high-frequency bands, which have been found to be more pleasant to the user than binary m-sequences (e.g., chaotic codes [8], 6-target optimum [9], superposition optimized pulses [10]). Recently, Gembler *et al.* [5] proposed the use of quintary m-sequences (i.e., m-sequences with 5 different values) encoded as different shades of gray, reaching similar performances (binary vs. quintary: 99.4%, 98.5% at 60 Hz, 97.6%, 97.5% at 120 Hz, 97.9%, 97.6% at 240 Hz) than binary m-sequences while being significantly less annoying for users, especially for 60 Hz refresh rates. However, they did not study the influence of different non-binary bases (i.e., varying the number of different sequence values) in the user's comfort, as they only tested their system with a quintary m-sequence. For a comprehensive review on the topic, refer to Martínez-Cagigal *et al.* [6].

The objective of this pilot study is to analyze the influence of p-ary m-sequences on the accuracy and users comfort while using a c-VEP-based speller. The following p-ary m-sequences will be studied: base 2 (i.e., binary, 63-bit), base 3 (80-bit), base 5 (124-bit) and base 11 (120-bit). A 16-target speller at 120 Hz presentation rate will be used to maximize users comfort.

2 Subjects

Three healthy users (HU, mean age: 27.3 ± 1.7 years) were included in this pilot study. EEG signals were recorded using sixteen active electrodes, placed on F3, Fz, F4, C3, Cz, C4, CPz, P3, Pz, P4, PO7, POz, PO8, Oz, I1 and I2; using Fpz as a ground and the earlobe as reference. A *g.USBamp* amplifier (g.Tec, *Guger Technologies*, Austria) with a sampling rate of 256 Hz was attached to a PC Intel Core i7-7700 @3.6GHz, 32GB RAM. MEDUSA® (www.medusabci.com), a general-purpose system to develop BCI paradigms and experiments in Python, was used to record the data via lab-streaming layer (LSL) protocol, display the paradigm and process the stimuli in real-time [11,12]. Of note, the c-VEP speller was displayed in a LED FullHD @144 Hz monitor and built in an Unity application that communicates with MEDUSA® via TCP/IP sockets to ensure exact synchronization between paradigm onsets and EEG registering. An external phototransistor was also used to measure refresh delays between top and bottom monitor lines.

3 Methods

3.1 *P*-ary m-sequences

M-sequences are pseudo-random codes generated by linear feedback shift registers (LFSR) that are almost spectrally flat and thus, nearly orthogonal to circularly shifted versions of themselves [6]. However, by definition, m-sequence lengths are restricted by the order r of the LSFR (i.e., the number of taps) and the sequence base p (i.e., number of different values or levels), so the length of the sequence will be $L = p^r - 1$ bits [6]. An interesting property is that combinations (except all zeros) of event subsequences of length equal or less than r are also nearly perfectly counterbalanced inside the code [13]. It is also important to highlight that m-sequences can only be obtained if the LFRS taps are coefficients of an primitive polynomial of degree r in the Galois Field with p elements, i.e. GF(p^r) [13]. For instance, a binary 63-bit m-sequence may be generated using a LFSR of length $r = 6$ and polynomial $x^6 + x^5 + 1$ (encoded with taps 110000), i.e. hereafter $\mathrm{GF}(2^6)_{<x^6+x^5+1>}$.

The generation of p-ary m-sequences is not trivial, though. Galois Fields cannot have an arbitrary number of elements, but only those fields in which p is a prime number satisfy the operations of multiplication, addition, subtraction and

Table 1. M-sequences used in this study.

	Base	**Order**	**Length (bits)**	**Polynomial**	**Seed**	**Duration (s/cycle)***
GF(2^6)	2	6	63	$x^6 + x^5 + 1$	1,1,1,0,1,0	0.525
GF(3^4)	3	4	80	$x^4 + 2x^3 + 1$	2,1,0,1	0.667
GF(5^3)	5	3	124	$3x^3 + 2x^2 + 1$	2,1,0	1.033
GF(11^2)	11	2	120	$3x^2 + x + 1$	9,0	1.0

* Calculated using a monitor refresh rate of 120 Hz.

division and are eligible to generate m-sequences [13]. Thus, a m-sequence with base p and length L can be only generated if a primitive polynomial with degree r over GF(p^r) exists. Although primitive polynomials over GF(2^r), GF(3^r) or GF(5^r) can be easily found in the literature [14], polynomials of higher bases are usually found using numerical linear algebra algorithms [15]. Table 1 shows the chosen m-sequences and their generation details, while figure 1 depicts their color encoding, temporal series and normalized autocorrelation function. Of note, the seed only determines the initial subsequence of the m-sequence. Since all possible subsequences are included inside the code, different seeds do not generate different m-sequences, but shifted versions of the same code. As shown in figure 1, m-sequences for $p > 2$ usually present occasional phase values in which they are highly anti-/correlated. Undeniably, these points must be avoided when assigning different delays to each command to prevent misclassifications [5].

3.2 Signal processing

EEG signals was pre-processed in real-time using a notch filter at 50 Hz to remove power line interference; as well as a filter bank over 1–60 Hz, 12–60 Hz and 30–60 Hz [6]. All these band-pass filters were 7th-order infinite impulse response (IIR) Butterworth filters. Then, a canonical correlation analysis (CCA) was used to compute the c-VEP templates for each command using a circular shifting approach. CCA finds spatial filters so that the correlation between linear projections of two signals $\boldsymbol{A}$ and $\boldsymbol{B}$ is maximized [6].

In training, $\boldsymbol{A} \in \mathbb{R}^{k \cdot N_s, N_c}$ are the multi-channel EEG epochs when looking at the command without lag for k cycles, while $\boldsymbol{B}^{N_s, N_c}$ are the same epochs averaged over the cycles, where N_s is the number of samples per cycle and N_c indicates the number of channels. From the returned spatial filters $\boldsymbol{W}_a \in \mathbb{R}^{N_c, N_c}$ and $\boldsymbol{W}_b \in \mathbb{R}^{N_c, N_c}$, only the ones that maximize the correlations between the projections $\boldsymbol{A}\boldsymbol{w}_a$ and $\boldsymbol{B}\boldsymbol{w}_b$ are used; i.e., first columns of $\boldsymbol{W}_a$ and $\boldsymbol{W}_b$, respectively. The averaged response is then projected to compute the main c-VEP template $\boldsymbol{x}_0 = \boldsymbol{B}\boldsymbol{w}_b$, where $\boldsymbol{x}_0 \in \mathbb{R}^{N_s, 1}$. Templates for the rest of commands (i.e., $\boldsymbol{x}_1, \boldsymbol{x}_2, \dots, \boldsymbol{x}_{16}$) are calculated by circularly shifting $\boldsymbol{x}_0$ according to their assigned lags [6]. Note that this procedure is repeated for each filter of the filter bank, ending up with three different sets of templates, where $\boldsymbol{X}^{(i)} = (\boldsymbol{x}_1^{(i)}, \boldsymbol{x}_2^{(i)}, \dots, \boldsymbol{x}_{16}^{(i)}), i = 1, \dots, 3$ [6].

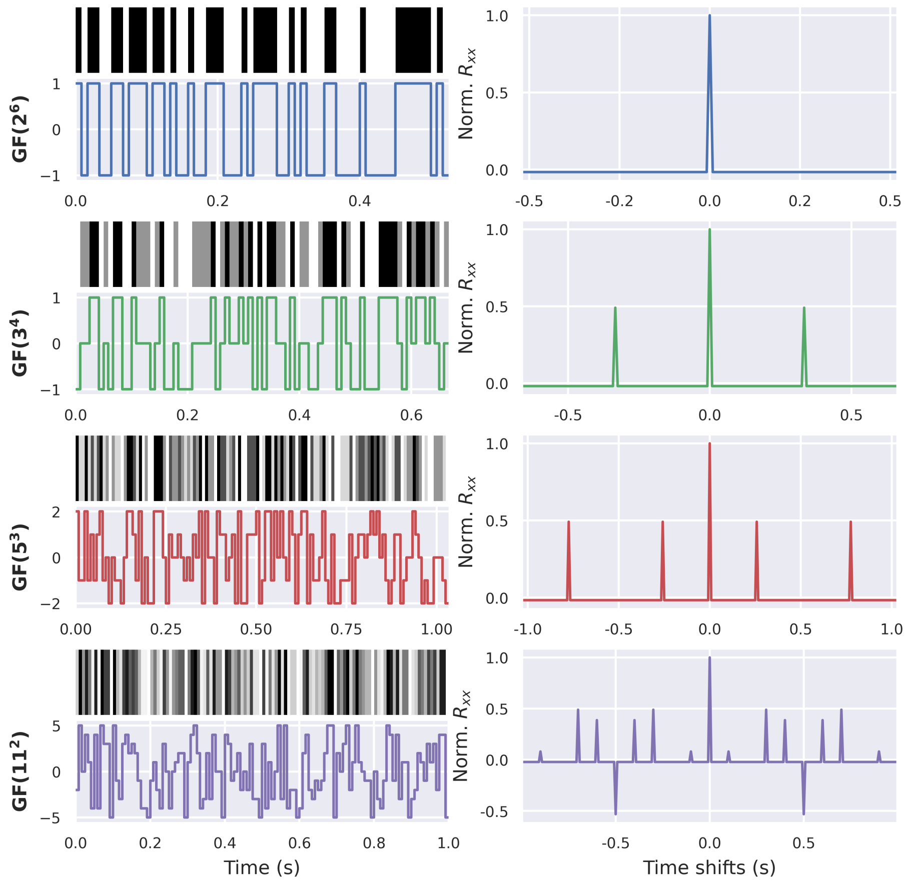

Fig. 1. P-ary sequences used in this study, from top to bottom: 63-bit GF(2^6), 80-bit GF(3^4), 124-bit GF(5^3), and 120-bit GF(11^2). For each one, color encoding, temporal code sequence and normalized autocorrelation (i.e., R_{xx}) functions are shown for a single cycle at a presentation rate of 120 Hz.

In online mode, multi-channel EEG epochs of a stimulation for k_t cycles are averaged and projected with $\boldsymbol{w}_b$ to obtain a spatially-filtered epoch, i.e. $\hat{\boldsymbol{x}} \in \mathbb{R}^{N_s,1}$. Then, the Pearson's correlation coefficient between $\hat{\boldsymbol{x}}$ and each of the templates $\boldsymbol{x}_1^{(i)}$ is averaged over filter banks, identifying the selected command as the one that reaches the maximal correlation value, i.e. $y = \arg\max_j [\sum_i \rho(\hat{\boldsymbol{x}}, \boldsymbol{x}_j^{(i)})]$, where $j = 1, \ldots, 16$. For further details, refer to Martínez-Cagigal *et al.* [6].

Following the approach of Nagel *et al.* [16], we also corrected the 'raster latencies'. Due to vertical blanking, pixel lines are refreshed from top to bottom, resulting in latency variations among different commands depending on their position on the screen. We used an external phototransistor to measure the delay

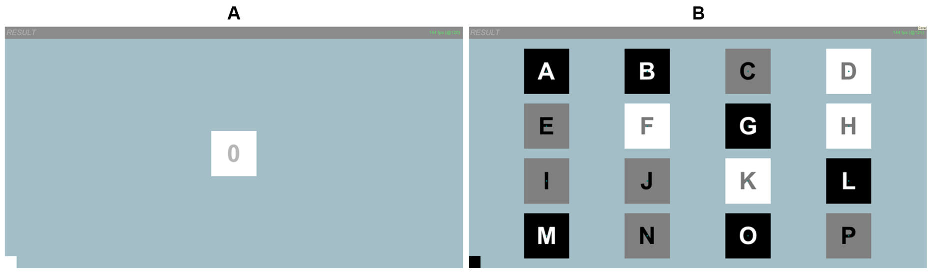

Fig. 2. A. Training matrix, which displayed the original m-sequence. B. Online matrix, where each of the 16 commands is modulated by a different shifted-version of the original m-sequence. In these examples, GF(3^4) was used and thus, three different tones encoded the m-sequence values.

between the first top line and the last bottom line, estimating a total delay of 7.92 ms (approx. 95% of the refresh rate) [16]. Thus, training templates $\boldsymbol{x}_j^{(i)}$ are delayed according to the display latency of the commands they belong to.

Finally, an online artifact detection algorithm was applied to correct noisy epochs. In training, the standard deviation of $\boldsymbol{A}$ for each channel across training k cycles is computed, i.e. $\sigma_{\boldsymbol{A}} \in \mathbb{R}^{1,N_c}$. In online mode, the same metric is computed for the test epochs $\hat{\boldsymbol{x}}$. Cycle-wise, a channel is interpolated with the averaged EEG of the nearest 3 channels if $\sigma_{\hat{\boldsymbol{x}}} > 3 \cdot \sigma_{\boldsymbol{A}}$ for that cycle. This method takes care of powerful non-stationary artifacts that can ruin the prediction, such as blinking or electrode-pops.

3.3 Evaluation protocol

Each user carried out a single session in which training and test trials of each of the m-sequences were recorded. For each m-sequence, training was performed with 20 trials and online mode was composed of 32 trials. Each trial was composed of 10 stimulation cycles. In training, users were asked to pay attention to a single command, which displayed the selected m-sequence without any lag. In online mode, users were asked to sequentially select each of the 16 commands in lexicographic order twice. Training and online c-VEP matrices are shown in figure 2. After the online mode, users fulfilled a questionnaire to reflect their subjective experience regarding visual discomfort of each m-sequence.

4 Results and discussion

Table 2 details the grand-averaged accuracies and ITRs across users for each of the evaluated m-sequences in function of the number of online cycles. In figure 3(A), a visual comparison of these results using 10 cycles per trial is depicted. Results of the qualitative questionnaire on visual eyestrain are also shown in figure 3(B).

Table 2. Grand-average online results across users.

	$\mathbf{GF}(2^6)$		$\mathbf{GF}(3^4)$		$\mathbf{GF}(5^3)$		$\mathbf{GF}(11^2)$		**Mean**	
k_t	Acc.	ITR	Acc.	ITR	Acc.	ITR	Acc.	ITR	Acc.	ITR
1	63.5%	202.3	80.2%	233.2	84.4%	163.0	84.4%	175.7	78.1%	193.6
2	91.7%	189.5	96.9%	155.5	96.9%	107.4	96.9%	107.7	95.6%	140.0
3	97.9%	148.3	99.0%	114.2	100.0%	77.4	99.0%	77.8	99.0%	104.4
4	100.0%	114.3	100.0%	90.0	100.0%	58.1	97.9%	56.8	99.5%	79.8
5	100.0%	91.4	100.0%	72.0	100.0%	46.5	99.0%	46.7	99.7%	64.1
6	100.0%	76.2	100.0%	60.0	100.0%	38.7	99.0%	38.9	99.7%	53.5
7	100.0%	65.3	100.0%	51.4	100.0%	33.2	99.0%	33.4	99.7%	45.8
8	100.0%	57.1	100.0%	45.0	100.0%	29.0	100.0%	30.0	100.0%	40.3
9	100.0%	50.8	100.0%	40.0	100.0%	25.8	99.0%	25.9	99.7%	35.6
10	100.0%	45.7	100.0%	36.0	100.0%	23.2	100.0%	24.0	100.0%	32.2

k_t: Number of test cycles, Acc.: accuracy (%), ITR: information transfer rate (bpm).

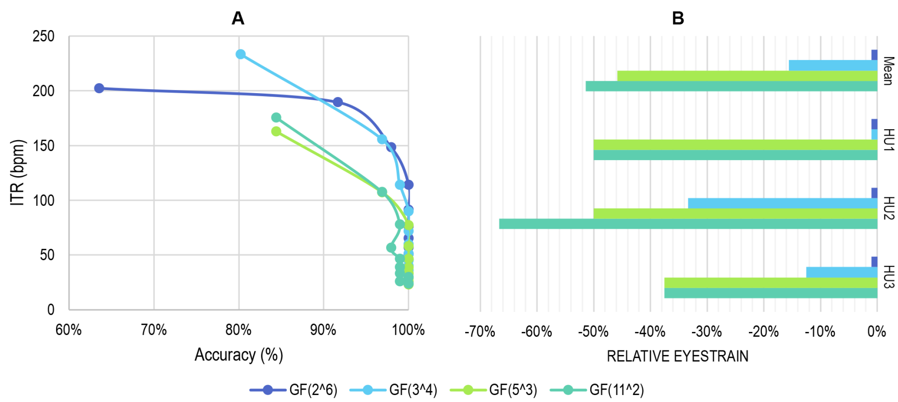

Fig. 3. A. Grand-averaged accuracies and ITR for each m-sequence (10 cycles/trial). B. Subjective eyestrain in relative percentage to the produced by the binary code, i.e. $\mathrm{GF}(2^6)$.

In terms of performance, 100% correct selections was achieved for all m-sequences using 10 cycles/trial. Differences arose when using a reduced number of cycles to reduce the time to perform a command selection, which also depends on the length of the m-sequence (see table 1). As shown, a 100% accuracy was achieved by $\mathrm{GF}(2^6)$ in 4 cycles (114.3 bpm, 2.1 s/trial), $\mathrm{GF}(3^4)$ in 4 cycles (90 bpm, 2.6 s/trial), $\mathrm{GF}(5^3)$ in 3 cycles (77.4 bpm, 3.1 s/trial), and $\mathrm{GF}(11^2)$ in 8 cycles (30 bpm, 8.0 s/trial). Interestingly, $\mathrm{GF}(2^6)$ showed a steeper slope in terms of performance for a low number of cycles compared to the p-ary m-sequences (see figure 3(A)), obtaining only 63.5% accuracy for 1 cycle/trial, while the rest exceeded 80%. Considering the trade-off between accuracy and speed, $\mathrm{GF}(2^6)$, $\mathrm{GF}(3^4)$ and $\mathrm{GF}(5^3)$ are all suitable to achieve very good performance in given amount of time. Although the use of $\mathrm{GF}(11^2)$ is perfectly viable, user HU2 had a selection error (31 correct out of 32), which caused the performance to drop to 99% from 5 cycles onward. However, as the length is similar to GF(5^3) and therefore ITR is almost equivalent, the preliminary results of this manuscript suggest using GF(5^3) instead in terms of performance.

Given that all *p*-ary sequences achieved suitable performance, the next step is to consider their influence on users comfort. As expected, the higher the base, the lower the user's perceived eyestrain. Thus, GF(11^2) was considered the least annoying m-sequence, followed by GF(5^3), GF(3^4) and finally GF(2^6); being perceived as 15.28%, 45.88%, and 51.39% less obtrusive in relative percentage than GF(2^6), respectively. Interestingly, some users did not perceive significantly different discomfort between certain m-sequences. For instance, HU1 considered GF(2^6) and GF(3^4), and GF(5^3) and GF(11^2) similar in terms of visual fatigue; and HU3 did not perceive a reduction in eyestrain from GF(5^3) to GF(11^2). Although the hypothesis that a higher base produces less visual eyestrain due to a reduction in overall perceived contrast seems to hold, further analyses with more subjects are required to give insight into the perceived annoyance in function of m-sequence base. Considering the balance between performance and annoyance, the use of GF(3^4) or GF(5^3) is recommended, although it depends on the user's sensitivity to strong visual contrasts.

These preliminary results are in accordance with the previous study by Gembler *et al.* [5], in which they compared the performance and user friendliness of two GF(2^6) and GF(5^3) m-sequences. Although both achieved similar results at 120 Hz monitor rate (binary: 97.6%, quintary: 97.5%), GF(5^3) was perceived as significantly less annoying that GF(2^6). Based on these results, we consider the use of *p*-ary m-sequences in state-of-the-art c-VEP-based BCIs to be promising for reducing visual fatigue.

Despite these positive results, further analysis on the topic should be encouraged as future lines of research. Firstly, increasing the sample size is essential to give more power to the comparison and allow statistical analyses between the results of different *p*-ary m-sequences. In this study, a total of 16 commands were used in online mode. The number of possible commands is a key aspect of circular shifting approaches, as they must fit into the m-sequence without falling into local cross-correlation maxima. For instance, including 36 commands (all letters and numbers) may not be feasible for m-sequences such as GF(2^6), GF(7^2) or GF(3^4). Analyzing the viability of different *p*-ary m-sequences in terms of the possible number of commands is an interesting future research line. Another study could also focus on studying the role of the number of training trials in achieving suitable online performance, or even use adaptive approaches [6]. In both this study and Gembler *et al.* [5], m-sequence levels were encoded with different shades of gray. Interestingly, different colors have been shown to affect EEG responses in both c-VEP and SSVEP-based systems [6]. Hence, another line of research would be to study the role of different color encoding for *p*-ary m-sequences. Furthermore, the extra dimensions provided by these *p*-ary m-sequences would not only allow the exploitation of color variations, but also other aspects such as stimuli sizes, apparent motions, or changing images; that have not yet been studied.

5 Conclusion

In this study, we analyzed the application of non-binary m-sequences as a more pleasant alternative than binary codes for c-VEP-based BCIs. M-sequences with different bases on GF(2^6), GF(3^4), GF(5^3) and GF(11^2) encoded with different shades of gray were studied. The results showed that the higher the base, the lower the visual fatigue perceived by the user. Although all of them were able to achieve 100% accuracy online, it was observed that the selection speed decreased slightly with increasing base due to the length of the m-sequences: 63-bit GF(2^6), 2.1 s/trial, 114.3 bpm; 80-bit GF(3^4), 2.6 s/trial, 90.0 bpm; 124-bit GF(5^3), 3.1 s/trial, 77.4 bpm; 120-bit GF(11^2), 8.0 s/trial, 30 bpm. Given the trade-off between performance and eyestrain, we conclude that the use of GF(3^4) or GF(5^3) is adequate to provide a reliable, comfortable, high-speed c-VEP-based BCI system. However, further studies are encouraged to increase statistical power and to analyze other aspects such as number of commands, color encoding and training duration.

Acknowledgments

This study was partially funded by projects PID2020-115468RB-I00, RTC2019-007350-1 and PDC2021-120775-I00 of 'Ministerio de Ciencia e Innovación/Agencia Estatal de Investigación' and European Regional Development Fund (ERDF); 0702_MIGRAINEE_2_E ('Análisis y correlación entre la epigenética y la actividad cerebral para evaluar el riesgo de migraña crónica y episódica en mujeres') of the European Commission and ERDF, and by 'CIBER en Bioingeniería, Biomateriales y Nanomedicina (CIBER-BBN)' through 'Instituto de Salud Carlos III' co-funded with ERDF funds. E. S.-V., S. P.-V. and D. M.-M. were in receipt of a PIF grant by the 'Consejería de Educación de la Junta de Castilla y León'.

References

1. Wolpaw, J., Wolpaw, E.W.: Brain-computer interfaces: principles and practice. OUP USA (2012)
2. Martínez-Cagigal, V., Santamaría-Vázquez, E., Gomez-Pilar, J., Hornero, R.: Towards an accessible use of smartphone-based social networks through brain-computer interfaces. Expert Systems with Applications **120**, 155–166 (2019). DOI 10.1016/j.eswa.2018.11.026
3. Santamaría-Vázquez, E., Martínez-Cagigal, V., Gomez-Pilar, J., Hornero, R.: Asynchronous Control of ERP-Based BCI Spellers Using Steady-State Visual Evoked Potentials Elicited by Peripheral Stimuli. IEEE Transactions on Neural Systems and Rehabilitation Engineering **27**(9), 1883–1892 (2019)

4. Bin, G., Gao, X., Wang, Y., Hong, B., Gao, S.: VEP-based brain-computer interfaces: Time, frequency, and code modulations. IEEE Computational Intelligence Magazine **4**(4), 22–26 (2009). DOI 10.1109/MCI.2009.934562
5. Gembler, F.W., Rezeika, A., Benda, M., Volosyak, I.: Five Shades of Grey: Exploring Quintary m -Sequences for More User-Friendly c-VEP-Based BCIs. Computational Intelligence and Neuroscience **2020** (2020). DOI 10.1155/2020/7985010
6. Martínez-Cagigal, V., Thielen, J., Santamaría-Vázquez, E., Pérez-Velasco, S., Desain, P., Hornero, R.: Brain–computer interfaces based on code-modulated visual evoked potentials (c-VEP): a literature review. Journal of Neural Engineering **18**(6), 061,002 (2021). DOI 10.1088/1741-2552/ac38cf. URL https://iopscience.iop.org/article/10.1088/1741-2552/ac38cf
7. Başaklar, T., Tuncel, Y., Ider, Y.Z.: Effects of high stimulus presentation rate on EEG template characteristics and performance of c-VEP based BCIs. Biomedical Physics and Engineering Express **5**(3) (2019). DOI 10.1088/2057-1976/ab0cee
8. Shirzhiyan, Z., Keihani, A., Farahi, M., Shamsi, E., GolMohammadi, M., Mahnam, A., Haidari, M.R., Jafari, A.H.: Introducing chaotic codes for the modulation of code modulated visual evoked potentials (c-VEP) in normal adults for visual fatigue reduction. PLoS ONE **14**(3), 1–29 (2019). DOI 10.1371/journal.pone.0213197
9. Behboodi, M., Mahnam, A., Marateb, H., Rabbani, H.: Optimization of Visual Stimulus Sequence in a Brain-Computer Interface Based on Code Modulated Visual Evoked Potentials. IEEE Transactions on Neural Systems and Rehabilitation Engineering **2**(c) (2020). DOI 10.1109/TNSRE.2020.3044947
10. Yasinzai, M.N., Ider, Y.Z.: New approach for designing cVEP BCI stimuli based on superposition of edge responses. Biomedical Physics and Engineering Express **6**(4) (2020). DOI 10.1088/2057-1976/ab98e7
11. Santamaría-Vázquez, E., Martínez-Cagigal, V., Hornero, R.: MEDUSA: una nueva herramienta para el desarrollo de sistemas Brain-Computer Interface basada en Python. Cognitive Area Networks **5**(1), 87–92 (2018)
12. MEDUSA: MEDUSA: a Python-based BCI framework (2022). URL www.medusabci.com
13. Buračas, G.T., Boynton, G.M.: Efficient design of event-related fMRI experiments using m-sequences. NeuroImage **16**(3 I), 801–813 (2002). DOI 10.1006/nimg.2002.1116
14. Mullen, G.L., Panario, D.: Handbook of finite fields, vol. 17. CRC Press Boca Raton (2013)
15. Di Porto, A., Guida, F., Montolivo, E.: Fast algorithm for finding primitive polynomials over GF (q). Electronics Letters **28**(2), 118–120 (1992)
16. Nagel, S., Dreher, W., Rosenstiel, W., Spüler, M.: The effect of monitor raster latency on VEPs, ERPs and Brain–Computer Interface performance. Journal of Neuroscience Methods **295**, 45–50 (2018). DOI 10.1016/j.jneumeth.2017.11.018. URL http://dx.doi.org/10.1016/j.jneumeth.2017.11.018